# Measurement of Pre-Sheath Potentials in Radio-Frequency Discharges

Sameer Ismail Farahat
The Islamic University of Gaza, P. O. Box 108, Gaza-Strip, Palestine

**Abstract**

In radio-frequency (RF) discharges, the pre-sheath potential is measured experimentally from the knee, which is located at the grid bias voltage or at the floating potential when the grid bias voltage is lower than the plasma potential. Plasma potential energy is constant at one value when the grid bias voltage is changed more negative than the plasma potential. Also, the post-sheath potential, or the positive pre-sheath potential is determined experimentally from the knee, which is located at the grid bias voltage plus an excess of energy $\epsilon$ when the grid bias voltage is higher than the plasma potential. The plasma potential is moving to higher values if the grid bias voltage changed to higher values than the plasma potential. We cannot measure these pre-sheath potentials using planar or cylindrical probes.

# 1 Introduction

The current-voltage (I-V) characteristic of Langmuir probe can provide information on ion and electron densities, the local space potential, and the isotropic electron energy distribution function. The current collected by the probe will be carried in the plasma by both ions and electrons, thus the I-V characteristic can yield information on both of the charge carriers. However, the basic Langmuir technique does not provide any means of distinguishing between the current contributions of the ions and electrons.

Information on energetic electrons is contained in the region of the I-V characteristic where the electrons are strongly retarded. In this regime the probe is often near the floating potential where the ion and electron currents are comparable, making it difficult to determine the electron energy distribution. The error due to ion collection can be partially compensated numerically by assuming a form for ion current. When the electron distribution is the object of the investigation often a linearized ion contribution is subtracted and approximated by a linear square fit to the probe current performed in a region below the floating potential [2]. This fact strongly limits the possibility of obtaining reliable data on the energetic electrons in spite of a strong technological requirement. It should be noted that it was believed that in order to avoid probe perturbation of the plasma, the probe was usually chosen cylindrical and as thin as possible, with dimension comparable with the Debye length, that is, in the range where the curvature of the ion characteristic cannot be neglected.

However, when the electron energy distribution function is required at high energies, the positive ion current must be eliminated from the measurements by the use of a gridded probe of two grids and a collector [3]. The spacing between the grid wires must be smaller than the Debye length; otherwise the plasma will squeeze between the wires and enter the probe. The gridded probe was not used by Ingram *et al* in their work to determine the plasma potential. Instead a cylindrical probe was ramped keeping the grid of the gridded probe at the working potential.

Bohm sheath criterion states that: "To give the ions the direct velocity $v_s \geq v_B = (k_B T_e/M_i)^{1/2}$, there must be a finite electric field in the plasma over some region, typically much wider than the sheath, called the pre-sheath"[4].

In RF discharges a compensation techniques (without phase correction)

developed and used with some success [5]. A similar compensation technique developed by Braithwaite *et al* (with phase correction) is used in this work which allows DC-type measurements to be made despite the presence of RF [6]. In this technique the RF potential across the plasma-probe sheath is minimized by feeding to the probe a synchronous external RF signal which is matched in amplitude and phase to the local space potential [7].

Our work proposes the gridded probe as a diagnostic technique to determine the plasma potential and any other DC potential in the plasma.

# 2 Apparatus

## 2.1 Vacuum Glass Vessel

The experimental work was performed in the apparatus shown in Figure 1. It consists of a high vacuum glass vessel, the cross-section of which has the form of a Maltese cross of height and width of 0.3 m. It is mounted on a table below which is the pumping equipment, diffusion and rotary pumps, which extract gas through the lower limb of the vessel. On the other three limbs there are grounded stainless steel flanges. The two 0.1 m diameter parallel disc RF electrodes are mounted in the vertical plane on horizontal support tubes which pass through a 1.3 cm diameter sliding vacuum Wilson seals in the end flanges, allowing both electrodes to be moved. The driven electrode was made of stainless steel.

The vacuum chamber is within a coaxial, open cage of six copper straps which connect the two main grounded flanges thus forming a Faraday cage. This results in a symmetrical and coaxial distribution of earth return current so minimizing radiated noise and stray inductance. A base pressure less than $10^{-3}$Pascal is obtained before argon gas is introduced into the vacuum vessel through a needle valve. Argon is used because it is chemically inert. During the experimental runs Pirani gauge is used to set the pressure between 0.5 Pascal, and 10 Pascal and Penning gauge is used to measure the pressure down to 0.1 Pascal [8].

## 2.2 The Gridded Probe

A gridded probe was constructed with a tantalum collector and one or

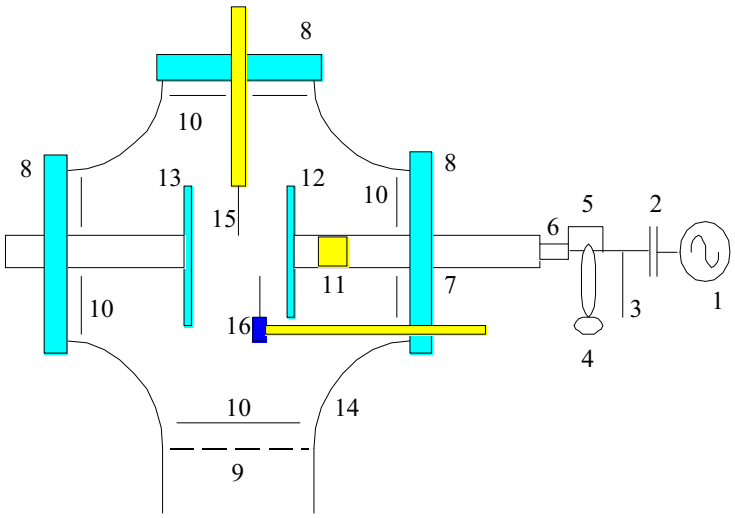


Figure 1: Experimental Apparatus: (1) RF amplifier, (2) blocking capacitor, (3) RF voltage probe, Tektronix P013A, (4) A.C. current probe, Tektronix P6022, (5) bridge for the RF guard, (6) RF guard, (7) grounded shield, (8) grounded flanges, (9) rounded grid to diffusion pump, (10) Teflon insulation, (11) ceramic insulation, (12) driven electrode, (13) grounded electrode, (14) glass vessel, (15) gridded probe, (16) cylindrical or planar probe.

two nickel grids each with 30 lines per millimeter and an optical transmission of 75%. The collector was made from 250-$\mu$m-thick tantalum sheet cut into a square with sides of length 0.5 cm as shown in Figure 2.

Field penetration is the penetration of the equipotential in the plane of the grid due to the effect of adjacent surface potentials (space charge introduces yet more problems). This could introduce significant errors to the measured distribution functions [9]. However, if the grid serves only to discriminate charge sign, it is only necessary to ensure that the minimum space potential at grid apertures is sufficiently large to reject the unwanted species. This can be achieved prior to recording experimental results by monitoring changes in the collector current as the grid potential is varied [10] [11]. It has been suggested that a double grid can be used to reduce this effect. However,

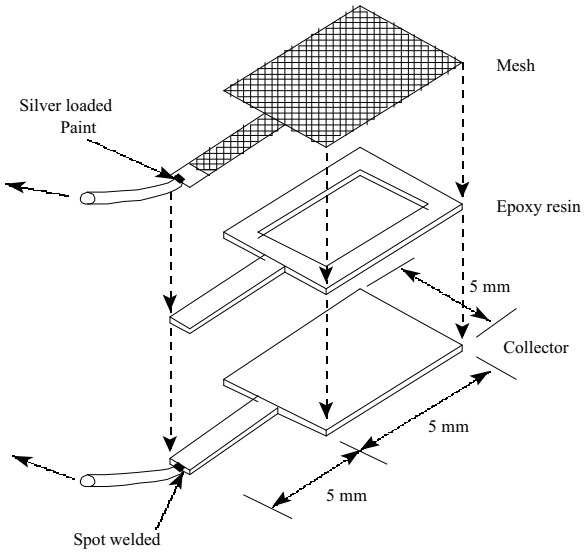


Figure 2: Schematic of the gridded probe construction.

two grids held at the same potential create a low-field region in which space-charge effects can be a major limitation. Therefore, it is necessary to apply a bias between the grids to insure that slow moving charges are swept out of the intervening space.

A more serious problem arising in using a probe with only one grid to measure electron energies is that the grid (held positive to reject ions) will draw an unacceptably large electron current from the plasma. This will result in a depletion of the local electron density which could change the local space potential, thus resulting in the distortion of the probe I-V characteristic near the plasma potential [12]. It is not sufficient to neglect the data from this region of the curve because the disturbance may be large enough to affect the nature of the entire discharge. Hence, as discussed above, the maximum area of the probe must be limited.

## 2.3 Acquisition-Obtaining a Probe Characteristic

The *PlasmaProbe* system hardware consists of an IBM compatible-PC hosting a 12-bit A/D - D/A expansion card and waveform generator. This card

provides signals to, and receives signals, from the *PlasmaProbe* amplifier unit which, in turn, drives the Langmuir probe itself, AEA Technology [13].

The voltage ramp is typically split into 1000 voltage steps with 24 samples taken at each step [14]. The basic waveform applied to the probe is a ramp followed by a plateau. During each ramp period the currents flowing in the probe circuit are measured to form parts of the characteristic. Negatively going ramps are immediately followed by positively going ramps and the data for each direction are stored separately.

Surface contamination of a Langmuir probe can begin to electrically isolate the probe from the plasma thus distorting the current-voltage characteristic. The plateau of the voltage waveform can be used to clean the probe *in situ* either through ion bombardment or Ohmic heating. Applying a large negative potential cleans the probe by ion bombardment so sputtering contaminant particles away from the probe. The probe is cleaned for 10 minutes prior to recording results by exposing the surfaces to ion bombardment from the plasma. The front grid and collector were held at -15, -20, and -60 volts, respectively.

# 3 Compensated Gridded Probe Experiment

A gridded probe of one grid and a collector, area = $10.3\times10^{-6}$ m$^2$ has been used to characterise an RF plasma generated between two parallel electrodes one of which was excited at 13.56 MHz, called the driven electrode, and the other was grounded. The area of the driven and grounded electrodes are equal, $A_d = A_g = 7.85 \times 10^{-3}$m$^2$. In the course of the experiment the chamber was filled with argon at a pressure of 0.5 Pascal. The electrode separation was fixed at 6 cm and the RF voltage on the driven electrode was 300 $V_{pp}$. The grid and the collector were separated by $6.1\times10^{-4}$ m. In order to reduce RF voltage between the plasma and the gridded probe, the probe was driven with RF signal by maximising the floating potential of the grid, the amplitude and the phase of which were chosen to match the oscillation in the plasma.

The orientations of the gridded probe inside the chamber is determined by the angle $\Theta$. For example, the orientation is at $\Theta = 0^\circ$ when the face of the gridded probe is facing the driven electrode. The probe current was collected by a gridded probe, of one grid only, oriented at $\Theta = 30^\circ$ (3 cm

away from the driven electrode). The driven electrode was excited with 300 $V_{pp}$. The RF in the plasma was externally compensated. The grid was biased at 0 V, 10 V, 20 V, 30 V, 40 V, 50 V, 60 V and 70 V respectively. In this configuration the grid of the gridded probe was actually negative or positive with respect to plasma potential.

Plasma potentials are detrmined from the inflection points of the probe current, which is developed in calculus [15]

**Definition 1 :** *If a function $I = f(V)$ changes concavity at a point $V_0$ in its domain (i.e., if it changes from concave down to concave up or vice-versa), then $f$ is said to have an inflection point at $V_0$. This will happen when the second derivative $f''(V)$ passes from positive to negative through the value zero [15].*

The inflection points can be determined easily from the crossing of the second derivative of the probe current as shown in Figure 3 to Figure 10.

# 4 Experimental Results

There are three regimes observed by biasing the grid of the gridded probe to obtain probe currents.

## 4.1 The First Regime of the Grid Bias

The first regime is that when the probe trace has three inflection points one of them is exactly at the grid bias voltage, Figure 3, 4.

Figure 3 shows that the second derivative is crossing from positive to negative at 0 V, which is identical to the grid bias. That is, the first inflection point determines the grid bias voltage. The second derivative is crossing from negative to positive at 8.4 V. The second inflection point at 8.4 V is only due to the continuity of the probe current. Finally, the second derivative is crossing from positive to negative at 20.3 V, which means that the third inflection point determines the plasma potential.

By biasing the grid at 10 V as shown in Figure 4 the second derivative crosses from positive to negative at 10 V which is identical to the grid bias. That is, the first inflection point determines the grid bias voltage. The second derivative crosses from negative to positive at 18.9 V. The second inflection

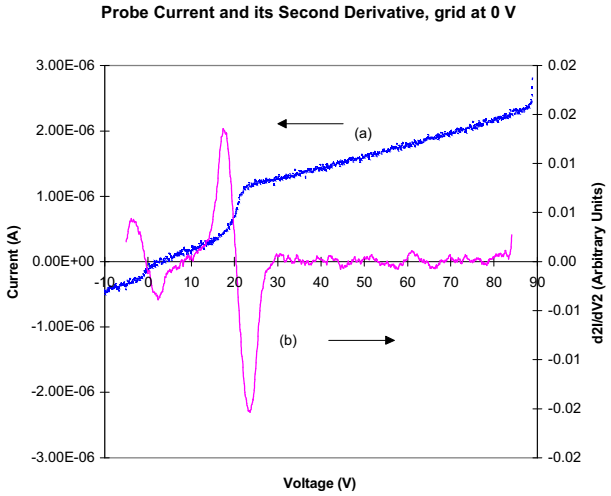


Figure 3: (a) The probe current, the grid was at 0 V. (b) The second derivative. There are three inflection points at 0 V, 8.4 V, and 20.3 V. The first inflection point determines the grid bias voltage at 0 V. The third inflection point determines the plasma potential at 20.3 V.

point at 18.9 V is only due to the continuity of the probe current. Finally, the second derivative is crossing from positive to negative at 20.5 V, which is due to the plasma potential.

It is observed that the probe current crosses the voltage axis at 5 V, which indicates that all the ions arriving at the grid pass through the grid to the collector during the probe bias. Also, it is clear that the third inflection point which determines the plasma potential is kept constant at 20.5 V.

This phenomena is observed if we left the grid bias at the floating potential. However, this phenomena is not observed if we bias the plasma by the grid and the I-V characteristic trace is obtained by planar or cylindrical probe.

From this regime we conclude that biasing the plasma with negative potential will not alter the plasma potential. Therefore, we have the following definition:

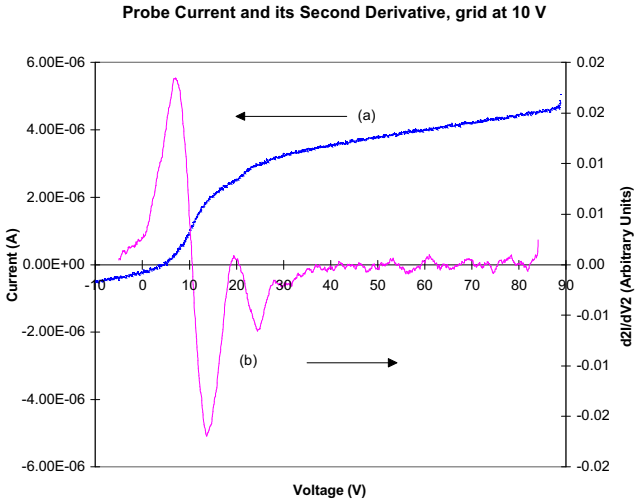


Figure 4: (a) The probe current, the grid was at 10 V. (b) The second derivative. There are three inflection points at 10 V, 18.9 V, and 20.5 V. The first inflection point determines the grid bias voltage at 10 V. The third inflection point determines the plasma potential at 20.5 V.

**Definition 2 :** *If the grid bias voltage is lower than the plasma potential then the plasma potential can be determined very accurately from the third inflection point. The fist inflection point, which is exactly at the grid bias voltage determines what we call the pre-sheath potential. The pre-sheath potential is more negative than the plasma potential.*

## 4.2 The Second Regime of the grid bias

The second regime is that when there is only one inflection point, usually very close to the grid bias.

By biasing the grid at 20 V, it is found that the crossing of the second derivative of the probe current is at 20 V, as shown in Figure 5. That is, the inflection point determines the grid bias voltage. There is no any other inflection point to determine plasma potential.

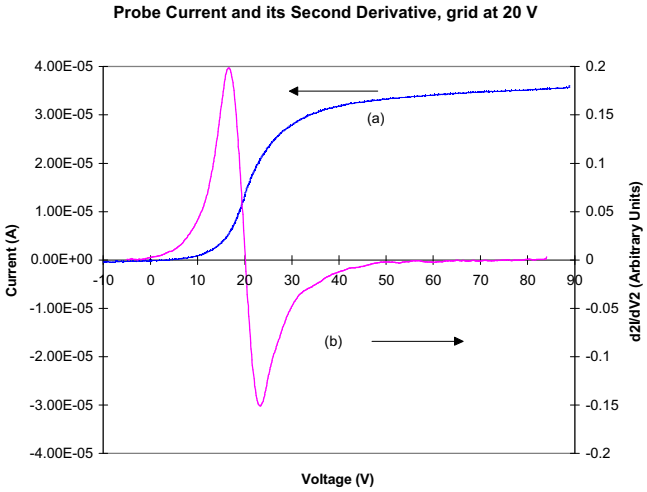


Figure 5: (a) The probe current, the grid was at 20 V. (b) The second derivative. There is only one inflection points at 20 V. This inflection point determines the grid bias voltage at 20 V. Also, this inflection point determines the plasma potential at 20 V.

## 4.3 The Third Regime of the grid bias

The third regime is observed when there is no ion current in the probe trace and the probe trace has three inflection points non of them are at the grid bias, but one of them is close to the grid bias.

By biasing the grid at $V_g = 30$ V, we find that there are three inflection points in the probe current as shown in Figures 6. The second derivative of the probe current crosses from positive to negative at 23.6 V, which is not identical to the grid bias. This inflection point determines the plasma potential. The second derivative crosses from negative to positive at 31.5 V. This inflection point is due to the continuity of the probe current. The second derivative of the probe current crosses from positive to negative at 35.1 V. This voltage is near to the grid bias voltage at 30 V. That is, the third inflection point determines the grid bias voltage, $V_g$, plus an excess of voltage, $V_\epsilon$. The third crossing of the second derivative from positive to

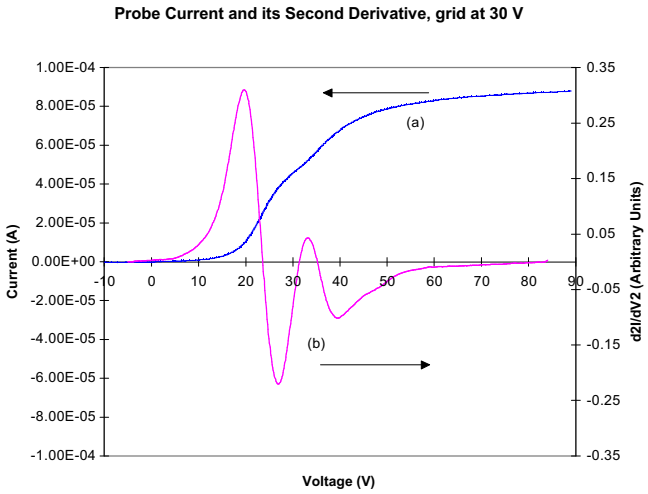


Figure 6: (a) The probe current, the grid was at 30 V. (b) The second derivative. There are three inflection points at 23.6 V, 31.5 V, and 35.1 V. The first inflection point determines the plasma potential at 23.6 V. The third inflection point determines the grid bias at 30 V plus an increment of energy $\epsilon = 5.1$ eV.

negative can be written as

$$V_S = V_g + V_\epsilon \tag{1}$$

where $V_S = 35.1$ V, $V_g = 30$ V and $V_\epsilon = 5.1$ V. Accordingly, we conclude that the grid is biased higher than the plasma potential. This is a good procedure to determine plasma potential and the excess of voltage $V_\epsilon$ very accurately. The probe current is flat between -10 V and 10 V, it indicates that no ions collected by the probe which means that all the ions are rejected by the grid and cannot pass to the collector during the probe bias.

Increasing the grid bias to 40 V, the three inflection points in the probe current are still exist as shown Figure 7. The second derivative of the probe current crosses from positive to negative at 26.2 V. The first inflection point determines the plasma potential. The second derivative of the probe current

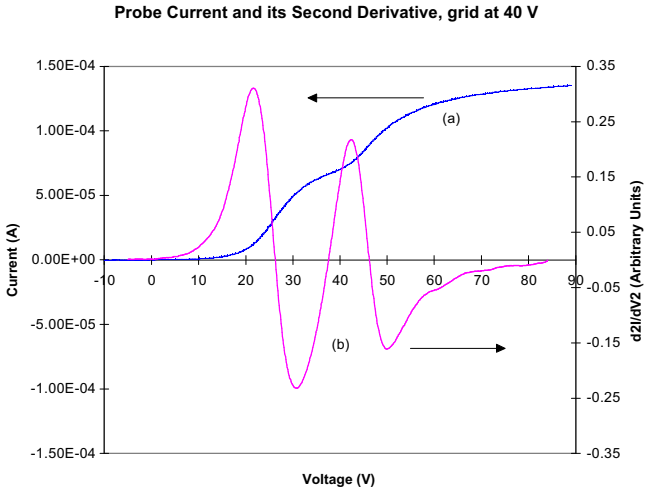


Figure 7: (a) The probe current, the grid was at 40 V. (b) The second derivative. There are three inflection points at 26.2 V, 37.6 V, and 45.6 V. The first inflection point determines the plasma potential at 26.2 V. The third inflection point determines the grid bias at 40 V plus an increment of energy $\epsilon = 5.6$ eV.

is crossing from negative to positive at 37.6 V which is due to the continuity of the probe current. The second derivative of the probe current is crossing from positive to negative at $V_S = 45.6$ V. This voltage is near to the grid bias voltage at $V_g = 40$ V plus an excess of voltage $V_\epsilon = 5.6$ V as in Eq. (1).

If the grid bias voltage is at 50 V, it is found that there are three inflection points in the probe current as shown in Figure 8. The second derivative of the probe current is crossing from positive to negative at 28.8 V, which is not identical to the grid bias, this inflection point determines the plasma potential. The second inflection point which is at 43.9 V is due to the continuity of the probe current. The third inflection point is at $V_S = 55.8$ V. This voltage is close to the grid bias voltage at 50 V. That is, the third inflection point determines the grid bias voltage, $V_g = 50$ V, plus an excess of voltage, $V_\epsilon = 5.8$ V.

Similarly when the grid bias is at 60 V, the three inflection points in the

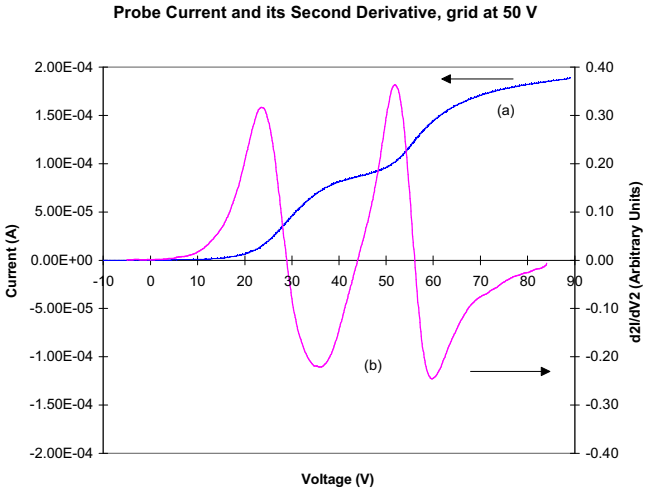


Figure 8: (a) The probe current, the grid was at 50 V. (b) The second derivative. There are three inflection points at 28.8 V, 43.9 V, and 55.9 V. The first inflection point determines the plasma potential at 28.8 V. The third inflection point determines the grid bias at 50.1 V plus an increment of energy $\epsilon = 5.8$ eV.

probe current are at 33.8 V, 52.2 V and 65.9 V as shown in Figure 9. The first inflection point determines the plasma potential at 33.8 V. The second inflection point at 52.2 V is due to the continuity of the probe current. The third inflection point at $V_S = 65.9$ V determines the grid bias voltage, $V_g = 60$ V, plus an excess of voltage, $V_\epsilon = 5.9$ V.

Finally, when the grid is at 70 V, it is found that there are three inflection points in the probe current as shown in Figure 10. The first inflection point determines the plasma potential at 43.7 V. The second inflection point at 62.1 V is due to the continuity of the probe current. The third inflection point at $V_S = 75.5$ V determines the grid bias voltage, $V_g = 70$ V, plus an excess of voltage, $V_\epsilon = 5.5$ V.

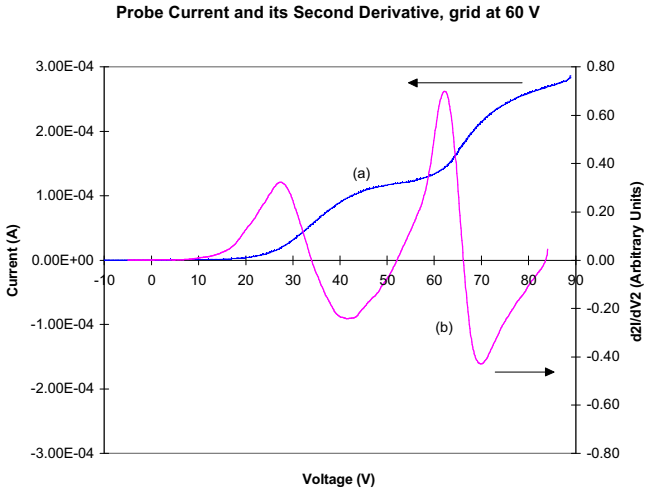


Figure 9: (a) The probe current, the grid was at 60 V. (b) The second derivative. There are three inflection points at 33.8 V, 52.2 V, and 65.9 V. The first inflection point determines the plasma potential at 33.8 V. The third inflection point determines the grid bias at 60 V plus an increment of energy $\epsilon = 5.9$ eV.

# 5 Discussion

Table 1 show the currents and voltages measured from the first and third infection points of the probe traces. In Table 1, $V_g$ is the grid bias voltage, $V_F$ and $I_F$ are the voltage and the current of the first inflection point, $V_S$ and $I_S$ are the voltage and current of the third inflection point. Also, Table 1 shows $V_\epsilon = V_S - V_g$ when the grid bias is higher than the plasma potential.

The studying of the inflection points, the knees in the probe current, of the third regime indicates that by increasing the grid bias by an increment of 10 V the plasma potential, which is determined from the first inflection point, is increasing from 23.6 V to 26.2 V, 28.8 V, 33.8 V and 43.7 V. That is, the increase in the plasma potential is not in an increment of 10 V.

The third inflection point which determines the grid bias $V_g$ plus an excess of voltage $V_\epsilon$ is increasing by an increment of 10 V plus $V_\epsilon$. It is clear that $V_\epsilon$

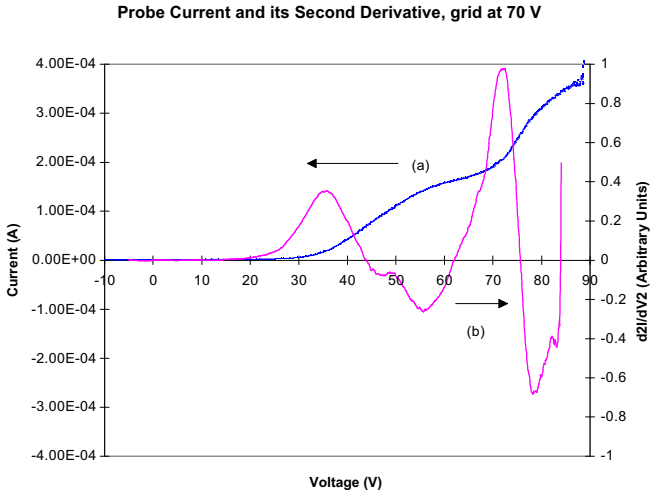


Figure 10: (a) The probe current, the grid was at 70 V. (b) The second derivative. There are three inflection points at 43.7 V, 62.1 V, and 75.5 V. The first inflection point determines the plasma potential at 43.7 V. The third inflection point determines the grid bias at 70 V plus an increment of energy $\epsilon = 5.5$ eV.

has a maximum value of 5.9 V, a minimum value of 5.1 V and the other three values for $V_\epsilon$ are fluctuating between the maximum and the minimum values. This suggests that the new parameter $V_\epsilon$ is not changing by increasing the grid bias voltage, but only fluctuating.

In order to understand the existence of $V_\epsilon$, let us assume the following different types of mechanism. One type is due to the secondary electron emission from the probe surface by the ions which accelerated by the grid. The positively charged ions are at the plasma potential and the grid is biased more positive than the plasma potential. This means that the grid and the ions will repel each other. That is, the ions will not pass through the grid to bombard the collector and cause the emission of the secondary electrons. From this physical mechanism we conclude that $V_\epsilon$ is not due to the emission of secondary electrons resulting from the bombardments of the probe surface by the ions. In fact, the ions have been repelled and have neither arrived at,

nor been collected by, the collector of the probe.

Table 1: The grid bias and the inflection points

| $V_g$(V) | $V_F$(V) | $I_F$(A) | $V_S$(V) | $I_S$(A) | $V_\epsilon$(eV) |
|---|---|---|---|---|---|
| 0 | 0 | $-1.8\times10^{-7}$ | 20.3 | $7.13\times10^{-7}$ | — |
| 10 | 10 | $1.11\times10^{-6}$ | 20.5 | $2.46\times10^{-6}$ | — |
| 20 | 20 | $1.32\times10^{-5}$ | 20 | $1.32\times10^{-5}$ | — |
| 30 | 23.6 | $2.41\times10^{-5}$ | 35.1 | $5.66\times10^{-5}$ | 5.1 |
| 40 | 26.2 | $3.14\times10^{-5}$ | 45.6 | $8.83\times10^{-5}$ | 5.6 |
| 50 | 28.8 | $3.87\times10^{-5}$ | 55.8 | $1.23\times10^{-4}$ | 5.8 |
| 60 | 33.8 | $5.37\times10^{-5}$ | 65.9 | $1.76\times10^{-4}$ | 5.9 |
| 70 | 43.7 | $6.59\times10^{-5}$ | 75.5 | $2.55\times10^{-4}$ | 5.5 |

The other type is due to the secondary electron emission from the probe surface due to the bombardment of energetic electrons, called primary electrons, accelerated by the grid. If an electron accelerated by the grid falls on the surface of the collector of the gridded probe, then either the electron returns to the plasma or penetrates into the solid and releases secondaries, a process often accompanied by X-ray emission [18]. For a secondary electron to be released the energy of the primary has to be larger than the work function $\phi$ of the solid. The spectrum of the emitted electrons is the sum of the secondaries and the reflected primaries and with slow electrons it is difficult to discriminate between them. In general a large fraction of the primaries is reflected from most surfaces. However, the angle of incidence is not equal to the angle of reflection, Snell's law, as in the case of a beam of light.

There are two theorems describe the emission of secondary electrons. The first is that when the primaries with energies above plasma potential are absorbed by the atoms, the atoms emit X-rays which in turn eject secondary electrons. The other is the emission to the transfer of energy from primaries to the valency electrons; or the interaction between the primaries and the free electrons in a Fermi level distribution whereby multiple elastic collisions then enable the secondaries to pass through the boundaries into the vacuum.

From the above discussion it is expected that the knee on the I-V characteristic will appear at the grid bias voltage, $V_g$. However, the experiments show that the knee is not at $V_g$, but at $V_g + V_\epsilon$. That is, the knee is not due

to secondary electrons as a result of primary electrons. Therefore, we have the following definition:

**Definition 3 :** *If the grid biased voltage is higher than the plasma potential then the first inflection point determines the plasma potential while the other inflection point which is at the grid bias voltage plus an excess of energy $\epsilon$ determines what we call the post-sheath potential, or the positive pre-sheath potential. The positive pre-sheath potential is more positive than the plasma potential.*

## 5.1 Conclusion

By biasing the grid of the gridded probe to obtain probe current it is found that there are three regimes. The first one is that when the grid is biased below the plasma potential. In this case, there are two knees, one knee is at the grid bias exactly while the other is at the plasma potential. The knee which is at the grid bias is called negative pre-sheath potential or pre-sheath. The pre-sheath exist if the grid is floating at the floating potential. The floating potential is usually lower than the plasma potential in our apparatus. The second regime is when the grid was close to the plasma potential. In this case there is only one knee. The third regime is when the grid is biased higher than the plasma potential. In this case there are two knees, the first one determines the plasma potential while the other is close to the value of the grid bias. In fact, the second knee in the third regime is at the grid bias plus an excess of energy $\epsilon$. This knee is called positive pre-sheath or post-sheath. In the third regime, plasma potential moving to higher values than that measured in the first regime.

### References


[**1**] Langmuir I., 1925, Phys. Rev. **26**, p 585.

[**2**] Allen J. E., Boyd R. F., and Reynolds P., 1959, Proc. Phys. Soc. **70**, p 297.

[**3**] Ingram S. G., Annaratone B. M. and Ohuchi M., 1990, Rev. Sci. Inst. **61**(7) p 1883.

[4] Bohm D., **The characteristics of Electrical Discharges in Magnetic Fields**, edited by Guthrie A. and Wakerling R. K., 1949, McGraw-Hill, New York.

[5] Wan A. S., Yang T. F., Lipschultz B. and LaBombard B., 1986, Rev. Sci. Inst. **57**, p 1542.

[6] Braithwaite N. St. J., Benjamin N. M. P. and Allen J. E., 1987, J. Phys. E **20**, p 1046.

[7] Boschi A. and Magistrelli F., 1963, Nuovo Cimento **29**, p 487.

[8] Delchar T. A., **Vacuum Physica and Technologies**, 1993, Chapman & Hall, London.

[9] Stephankis S. and Bennet W. H., 1968, Rev. Sci. Inst. **39**. p 1714.

[10] Ingram S. G. and Braithwaite N. St., 1988, J. Phys. D **21**, p 1496.

[11] Ingram S. G., and Braithwaite N. St., 1988, Mat. Res. Soc. Symp. Proc. Vol. 117.

[12] Okada.,1958, J., Phys. Soc. Jpn. **13**, p 1212.

[13] AEA Technology, **PlasmaSoft Scientific 1.00**, 1993, User's Guid.

[14] Hardware Manual, **PlasmaProbe Scientific**, 1994, UKAEA.

[15] Jonson J. M., **Calculus Theory and Application in Technology and Physical and Life Sciences**, 1987, ELLIS Horwood Limitede, Chichester.

[16] von Engle A., **Ionized Gases**, 1994, AIP Press, New York.